atmosphere

MDPI

Article

Analysis of Synergistic Effects of Cold Source and East Asian Winter Wind on Air Pollution in Typical Regions of China in Winter

Yanjun Li [1,2], Xingqin An [1,*], Baozhen Wang [3,*], Jiangtao Li [1] and Chao Wang [1]

[1] Chinese Academy of Meteorological Sciences, Beijing 100081, China; dionysusr@icloud.com (Y.L.); lijt15@lzu.edu.cn (J.L.); chaowang0920@163.com (C.W.)
[2] School of Atmospheric Sciences, Chengdu University of Information Technology, Chengdu 610225, China
[3] Green Intelligence Environmental School, Yangtze Normal University, Chongqing 408100, China
* Correspondence: anxq@cma.gov.cn (X.A.); 20170076@yznu.edu.cn (B.W.)

Abstract: This paper collects and analyzes the 1954–2017 monthly average reanalysis data from the U.S. National Centers for Environmental Prediction/National Center for Atmospheric Research (NCEP/NCAR), the 1954–2017 haze days observation data from the National Meteorological Information Center/China Meteorological Administration (NMIC/CMA) and the $PM_{2.5}$ daily average mass concentration data in 2013–2017 from the China Air Quality Online Monitoring Platform. The atmospheric apparent heat source Q_1 (negative Q_1 means cold source in winter) over the Tibetan Plateau in December of 1954–2017 is estimated based on thermodynamic equations, and the East Asian winter monsoon index (EAWMI) is calculated. In addition, the discrepancies of the air quality among China's five typical regions (Beijing–Tianjin–Hebei, Fen-Wei Plain, Yangtze River Delta, Pearl River Delta and Sichuan-Chongqing regions) under the joint influence of the Q_1 and EAWMI are studied. Results show that when it is a strong cold source year, abnormal downdrafts and "temperature inversion covers" occur in areas far from the high terrain, resulting in increased pollution, while the opposite is true in weak cold source years. In strong EAWMI years, there is an abnormal northerly sinking cold flow in the lower layers of mid-high latitudes, which increases the pollution in the area south of 30° N, and the opposite is true in weak EAWMI years. Affected by the combined activities of the Q_1 and the EAWMI, the meteorological conditions of the five typical regions are different, and thus present different air pollution characteristics.

Keywords: apparent heat source Q_1 on Tibetan Plateau; East Asian winter monsoon; air pollution; circulation background; typical regions of China

Citation: Li, Y.; An, X.; Wang, B.; Li, J.; Wang, C. Analysis of Synergistic Effects of Cold Source and East Asian Winter Wind on Air Pollution in Typical Regions of China in Winter. *Atmosphere* **2022**, *13*, 1162. https://doi.org/10.3390/atmos13081162

Academic Editors: Regina Duarte and Patricia K. Quinn

Received: 19 May 2022
Accepted: 15 July 2022
Published: 22 July 2022

1. Introduction

With the acceleration of industrialization and urbanization, China has been impacted by air pollution which has occurred frequently during late autumn and winter in economically developed areas of middle and eastern China in the past two decades [1,2]. Although air quality is determined by large changes in pollutant emissions, it is also affected significantly by the dynamic and thermodynamic impacts of weather and climate [3], especially in winter when pollution is the most frequent. There are strong climate systems over China, including the East Asian winter monsoon and the cold source of the Qinghai-Tibet Plateau. The strength of these systems affects the weather circulation in China [4–6] which, in turn, has an impact on pollution [7].

Since the 1950s, Yeh at al. [8], Flohn [9] and other scientists have conducted a lot of research on the effect of Tibetan Plateau terrain on atmospheric motion. The influence of the plateau on atmospheric circulation is mainly related to two aspects. The first is the mechanical blocking effect of plateau on atmospheric motion. All of the local circulations, long waves and even super-long waves are affected by topography. Such effects are mainly

the results of the airflow climbing by terrain forcing. The climbing or circumfluence of the airflow is related to the shape of the terrain, and where the terrain is long in the north–south direction, there is more climbing air. Of course, this is also associated with the structure of the airflow crossing the terrain [10–14]. Charney et al. [15] used numerical experiments for the first time to prove that the existence of the Tibetan Plateau and Rocky Mountains is an important reason for the formation of mid-latitude mid-tropospheric atmospheric circulation in winter. On the other hand, thermal effect plays an important role in the formation of the winter Mongolian high pressure and the summer Indian low pressure in Asia, thus leading to the development of the East Asian monsoon [16]. The monsoon is not only controlled by the sea–land thermal contrast, but the zonal asymmetric non-adiabatic heating and the large topography also significantly impacts the monsoon. Thus, the thermal effect of the Tibetan Plateau strengthens the thermal contrast between sea and land. Hahn D G et al. [17] compared model simulation results with mountains and without mountains by numerical simulation, finding that only when the information of Tibetan Plateau is put in the model can the monsoon climate extend further northward into the Asian continent, affecting the atmospheric circulation in East Asia.

It can be seen that the high terrain on the continent will affect the changes of the monsoon circulation. Li Gen et al. [18] further calculated the heat source value Q_1 of the Qinghai-Tibet Plateau located in East Asia using 1979–2014 data and its impact on the Chinese circulation and precipitation in North China in the following year. They pointed out that one of the causes for summer monsoon is the thermal difference between land and sea. When the heat source of the Tibetan Plateau is weak, the thermal difference between the sea and land becomes small, and the East Asian summer monsoon will be weaker, which is not conducive to the northward transport of water vapor. Similarly, when the heat source of the Tibetan Plateau is strong in the earlier stage, the thermal difference between the land and the sea will be larger. Accordingly, the East Asian summer monsoon tends to be stronger and abnormal, bringing a lot of water vapor northward. Similarly, the strength of cold sources in winter may also affect the winter monsoon.

Changes in atmospheric heat sources can influence the strength of the monsoon. In winter, the East Asian monsoon is a deep circulation system, which has an important impact on the winter atmospheric circulation. Gao Hui [19] used the reanalysis data to compare and analyze four kinds of East Asian winter monsoon indexes, finding that they all showed the characteristics of "strong (weak) winter monsoon year, strong (weak) lower Siberian high pressure, deep (shallow) Aleutian low pressure, strong (weak) subtropical northerly airflow, low (high) temperature in the subtropical East Asia, deep (shallow) middle East Asian trough and strong (weak) high-level subtropical westerly jet".

The change of monsoon can affect the change of atmospheric circulation and the distribution of pollutants. Based on the Terra satellite inversion data from March 2000 to March 2017, Ma et al. [20] found that the average winter AOD in eastern China has a good correlation with climatic elements, and the abnormally high AOD value in eastern China is associated with unusual low wind speed. This negative correlation is most obvious in North China: namely, when the AOD is abnormally high (low), the surface wind speed in North China is small (large) while the surface wind speed in Jianghuai region is large (small).

The method of Xu et al. [21] was used by Wang et al. [14] to calculate the sliding correlation between the atmospheric heat source intensity in the selected area of the eastern Tibetan Plateau during the springs of 1948–2002 and the East Asian summer monsoon index. The sliding window length was 23 years. They found that the winter monsoon has a significant impact on the atmospheric heat source anomalies on the Tibetan Plateau in spring. A weak winter monsoon is advantageous to a stronger spring thermal index of the plateau, while a strong winter monsoon is conducive to a weaker thermal index of the plateau in spring. This shows that the atmospheric heat source is also associated with the changes of monsoon strength.

In our previous research, we analyzed the interdecadal variation of the thermal effect of the Tibetan Plateau and the correlation between the apparent heat source Q_1 and the

air pollution in China [22]. By taking the strong and weak years of thermal effects, we made a comparative analysis on the difference of atmospheric circulation in strong and weak years and its influence on pollutant diffusion, and at the same time carried out a similar analysis on the winter monsoon in East Asia [23]. In this paper, we discuss how the air pollution in different regions of China changes when considering the influence of the Tibetan Plateau thermal effect and the East Asian winter monsoon, and investigate the causes for its occurrence.

2. Materials and Methods

This paper attempts to explore the climate system that exists over East Asia, i.e., the Qinghai-Tibet Plateau cold source and the East Asian winter monsoon, and how their strength changes will affect the weather circulation and pollution conditions in typical polluted areas in China. We collected long-term data, including $PM_{2.5}$, haze day data and meteorological data, to qualitatively analyze the relationship between EAWMI/Q_1 and pollution.

2.1. Data

This article uses the 1954–2017 NCEP/NCAR global reanalysis data, including geopotential height, temperature, wind speed and vertical velocity, with 17 layers in vertical direction and horizontal resolution of 2.5° × 2.5°.

The $PM_{2.5}$ mass concentration data are from the China Air Quality Online Monitoring Platform, which conducts secondary verification and statistics on the real-time observation data of 367 cities across the country provided by the China Environmental Monitoring Center, and finally releases daily air quality data for each city. This article selects its daily $PM_{2.5}$ mass concentration data from 2013 to 2017, including 1498 sites across the country, picking out 902 sites with continuous observation data for analysis.

The haze day data are from the latest *Special Dataset for Haze Days* (V1.0) [24], compiled and updated by the National Meteorological Information Center (NMIC), China Meteorological Administration (CMA) in 2018. The dataset includes the daily values of haze weather phenomena (including fog, mist and haze) observed by basic, benchmark weather stations and general weather stations in China, timing visibility, relative humidity, wind direction and other observations at four standard times per day (00:00, 06:00, 12:00, 18:00 UTC). It has been subjected to quality control of thresholds (or allowable values), internal consistency and spatial consistency. In this paper, 2444 sites with good data integrity from 1958 to 2017 are selected for research.

2.2. Atmospheric Apparent Heat Source Q_1

At present, there are two main methods for calculating atmospheric heat sources. One is the "positive algorithm", also known as the "direct algorithm", which uses observation data to calculate sensible heat, net radiation, and condensation latent heat, and the sum of the three is taken as the atmospheric heat source. The other is the "inverse algorithm" or "indirect algorithm", which, using the conventional data such as wind, temperature and geopotential height, adds the terms of the local change of potential temperature on isobar, temperature advection and vertical temperature change through Formula (1), and then performs vertical integration getting Formula (2) with the atmospheric heat source <Q_1> and the unit being W/m^2 or K/d. The calculation methods and data can cause uncertainty in the results. The "positive algorithm" can only obtain the entire heat source layer, while the "inverse algorithm" can obtain the vertical structure of the heat source, but the accuracy of the results depends on the accuracy of the reanalysis data [25–27].

This study intends to use the "inverse algorithm" to calculate the apparent heat source of Tibetan Plateau. The adopted apparent heat source Q_1 formula [28] is:

$$Q_1 = c_p \left[\frac{\partial T}{\partial t} + V \cdot \nabla T + \left(\frac{p}{p_0} \right)^k \omega \frac{\partial \theta}{\partial p} \right] \quad (1)$$

where Q_1 is the apparent heat source of each layer, T is temperature, ω is the vertical velocity of the P coordinate, p_0 is 1000 hPa, θ is the potential temperature, $R = 287$ J/(kg·K), $c_p = 1005$ J/(kg·K), $\kappa = R/c_p = 0.286$, R and c_p are the dry air gas constant and the constant pressure specific heat V as horizontal wind vector. By Formula (1), the Q_1 of each isobaric surface layer can be calculated.

The vertical integral value of the atmospheric apparent heat source can be expressed as:

$$\langle Q_1 \rangle = \frac{1}{g} \int_{p_t}^{p_s} Q_1 dp \tag{2}$$

where $\langle Q_1 \rangle$ is the apparent heat source of the entire layer, P_s and P_t are surface pressure and atmospheric top pressure (100 hPa), respectively, and g is the gravitational acceleration. Take integral value of the whole-layer apparent heat source Q_1 over the Tibetan Plateau (75°–100° E, 27.5°–37.5° N) in December when the cold source is the strongest to represent the thermal effect of the Qinghai-Tibet Plateau in winter, and standardize the 1954–2017 Tibetan Plateau apparent heat source Q_1. With plus or minus 1.2 as metric, years with an index less than −1.2 are determined as strong cold source years and the years meeting the criteria are 1959, 1960, 1965, 1996, 1997, 2007, 2011, 2013 and 2014. Then, the years with an index greater than 1.2 are grouped into weak cold source years, which include 1956, 1967, 1968, 1974, 1986, 1989, 2005 and 2010.

2.3. East Asian Winter Monsoon Index

Chinese meteorologists have used many approaches to define the East Asian Winter Monsoon Index (EAWMI). Here, the winter monsoon index I_{Sun} proposed by Sun Baimin et al. [29] is adopted, the average 500 hPa geopotential height over the East Asian trough region (30°–45° N, 125°–145° E) in December is chosen to represent the winter East Asian trough (disturbance) activity, and the I_{Sun} index is taken as a negative from its original definition; then. the high index can correspond to the strong East Asian winter monsoon, which is convenient for our discussion in the following paragraphs. According to the selected December I_{Sun} index that accounts for the strength of the winter monsoon, the East Asian winter monsoon index during 1958–2017 is standardized, with plus or minus 1 as the metric. Years with an index greater than 1 are considered to be strong winter monsoon years, including 1960, 1967, 1969, 1973, 1980, 1983, 2005, 2010 and 2014, while years with an index less than −1 are considered to be weak winter monsoon years, which are 1978, 1979, 1986, 1991, 1997, 2004, 2006, 2015 and 2016.

In terms of research methodology, the methods of correlation analysis and synthesis analysis are adopted in this article.

2.4. Atmospheric Circulation over the Tibetan Plateau

Referring to previous studies on the Tibetan Plateau [11], we made a basic schematic diagram (Figure 1) of the atmospheric circulation situation near the plateau. The gray columns in the figure represent the high terrain of Tibetan Plateau, and the red arrows account for Hadley cell, Ferrel cell and high-level westerly jet. The yellow arrow is the detouring flow of the westerly wind passing by the plateau terrain from the west. The north branch bypasses the Tianshan Mountains at 500 hPa and then turns southward, producing a powerful Xinjiang high-pressure ridge (the north branch at 700 hPa flows around the east side of the main body of the plateau, namely the leeward slope, generating an anticyclone system, known as Lanzhou small high pressure). The south branch passes through the Indo-Pakistan continent and turns to the north after crossing the Bay of Bengal, forming a broad trough of low pressure in the Bay of Bengal (at 700 hPa the south branch flows around the leeward slope of the plateau and forms a cyclonic system, called the southwest vortex). Therefore, over the western half of the main body of the plateau there are diverging airflows from the branches, while over the eastern half there are converging airflows. The orange arrow is the climbing airflow passing through the Tibetan Plateau. A cold high pressure exists in the middle and upper levels above the Tibetan Plateau, and the green

airflow is a cold high-pressure anticyclone. When the cold high pressure is strong enough, the anticyclone strengthens, causing the convergence and uplift of the lower airflow. The blue arrow represents the East Asian winter monsoon airflow.

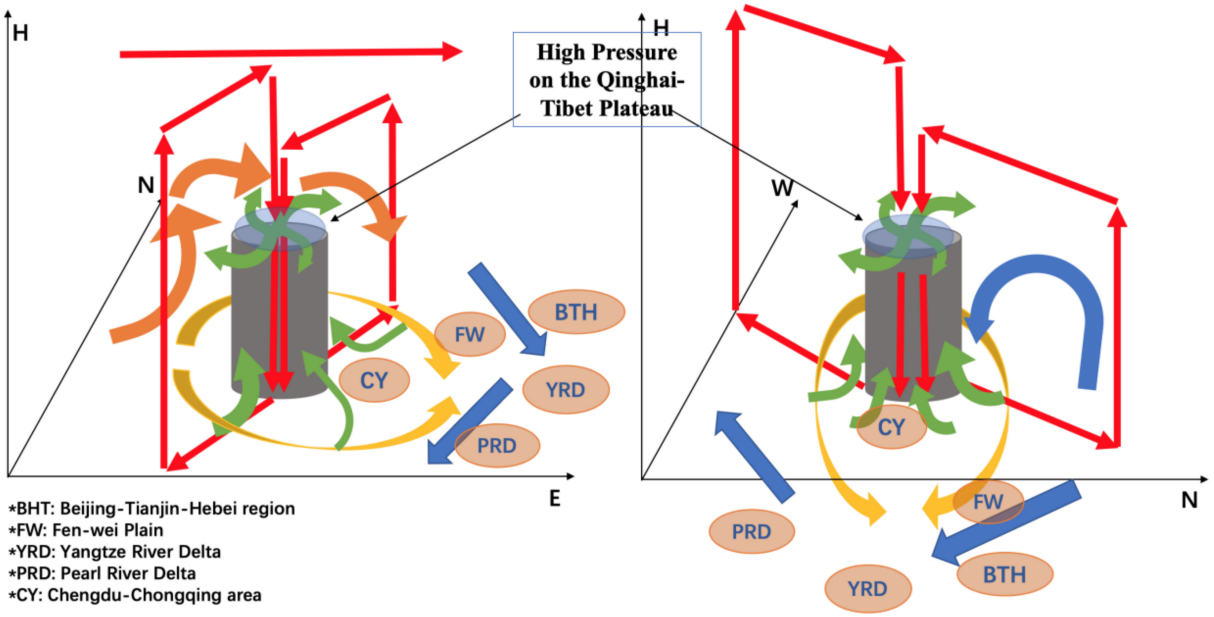

Figure 1. Overview of atmospheric circulation over and around the Tibetan Plateau.

The oval-shaped signs with letters in the picture represent five typical polluted urban agglomerations in China. The air quality in different regions is affected by geographical terrain, weather and pollution sources, and is also affected by the development of China's economy. Constrained by development, cities in different regions are increasingly densely distributed, and the atmosphere interacts with each other. Therefore, the pollution situation between some regions and cities shows a certain regularity. The typical pollution area in China in winter is Beijing–Tianjin–Hebei, Fen-Wei Plain, Yangtze River Delta, Pearl River Delta and Sichuan-Chongqing regions, so we take these as the main research objects to explore the impact of winter EAWMI and Q_1 on their pollution changes.

3. Results

3.1. Circulation Differences between Strong and Weak EAWMI/Q_1 Years

The Tibetan Plateau acts as a strong cold source in winter, which can cause the Hadley cell in the Southern Hemisphere to sink and extend to the northern plateau, thereby greatly strengthening the average meridional Hadley cell in the Northern Hemisphere in winter [30]. Then, under the year patterns with strong, weak cold sources, or strong, weak monsoons, how will the atmospheric circulations in the vicinity of the Tibetan Plateau and its eastern region vary? To respond to this question, we present the following discussion.

The strong and weak cold source years on the Tibetan Plateau and the strong and weak winter monsoon years in East Asia are selected for composite analysis, as shown in Figure 2. On the East Asian winter monsoon strong and weak year difference chart (left), we find the wind field and geopotential height field from 850 hPa to 700 hPa; the geopotential height of East Asia decreases in strong winter monsoon years, corresponding to the deepening of East Asian trough; and the increase of geopotential height in Siberia region matches with the strengthening of the Mongolian high. However, in Northeast China, North China, East China and South China, more obvious northward abnormal airflows are found, and the strengthening of northerly winds is in favor of the transport of pollutants to the south, while in the strong winter monsoon years over the Chengdu-Chongqing region, there exist abnormal easterly winds, conducive to the transport and accumulation of pollutants on the east side into the basin.

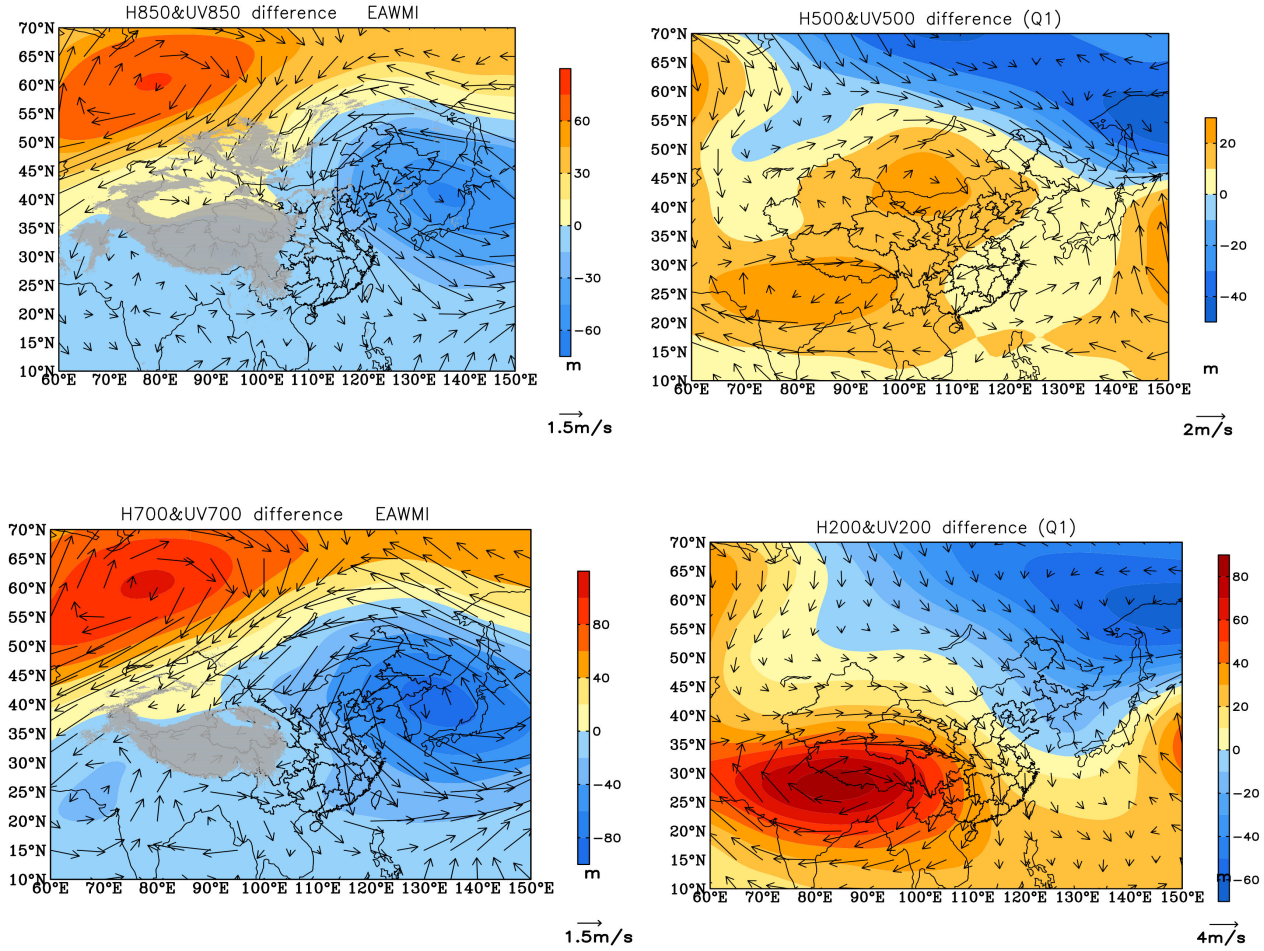

Figure 2. Wind and geopotential height at 850 hPa (**upper left**) and 700 hPa (**bottom left**) in strong and weak winter monsoon years; wind and geopotential height in strong and weak cold source years on the Tibetan Plateau at 500 hPa (**top right**) and 200 hPa (**bottom right**) (shaded areas are terrain corresponding to altitude).

On the cold source strong and weak year difference chart (right), the wind field and geopotential height field from 500 hPa to 200 hPa show that, over the Tibetan Plateau, the geopotential height increases significantly and there are abnormal anticyclone flows in the strong years of cold source, which proves that when cold sources on the Tibetan Plateau are strong, the cold high pressure on the plateau intensifies, causing even stronger anticyclone flow. The westerly wind flowing around the north side of the plateau strengthens, but the westerly flow around the south side weakens. Simultaneously, there is a low-pressure system over Kazakhstan, and there are obvious southwesterly winds in the southern Qinghai-Tibet Plateau and Nepal, which are consistent with Zhang et al. [31]. Such meteorological circulation conditions are conducive to the transport of pollutants from India and surrounding areas to the Qinghai-Tibet Plateau.

3.2. Composite Patterns of the Strong, Weak EAWMI Year and the Strong, Weak Q_1 Year on Tibetan Plateau

The standardized East Asian Winter Monsoon Index *EAWMI* (I_{Sun}) for the December of 1958–2017 and the time series for negative Q_1 are drawn as a time series diagram, as shown in Figure 3. The positive value represents the strong winter monsoon year (cold source year), and the negative value indicates a weak winter monsoon year (cold source year).

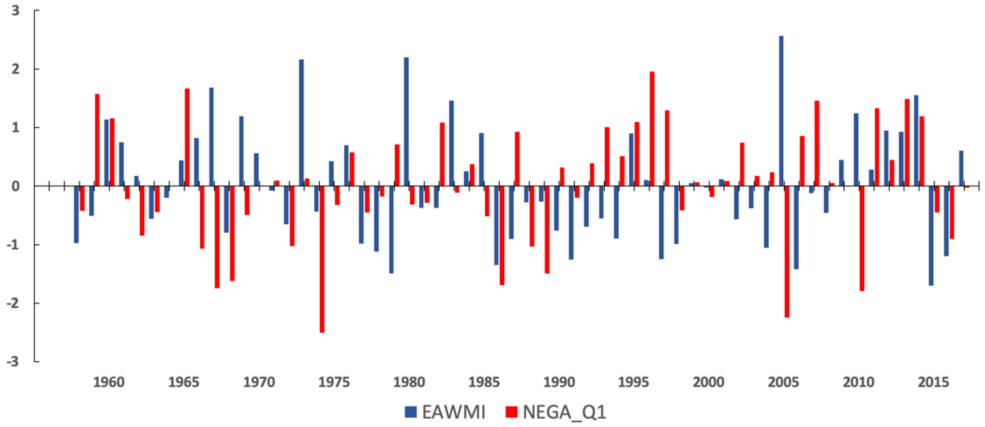

Figure 3. Time series of the standardized December East Asian Winter Monsoon Index *EAWMI* (I_{Sun}) during 1958−2017 and the negative values of Q_1.

We combine different strong and weak winter monsoon years with different strong and weak cold source years into four types, namely strong winter monsoon–strong cold source year type (2013 and 2014), strong winter monsoon–weak cold source year type (2010 and 2017), weak winter monsoon–strong cold source year type (2006 and 2008), and weak winter monsoon–weak cold source year type (2015 and 2016). Table 1 shows the details, in which +/− express the strong or weak signs with the values in brackets indicating strong or weak values. For example, in 2006, the cold source index of that year is 0.8543, which means it is a strong cold source year, whilst the winter monsoon index is −1.4221, indicating it is a weak winter monsoon year. The years 2008 and 2006 share the same year pattern, belonging to a strong cold source–weak winter monsoon year type; however, the cold source index for 2008 is 0.0531, weaker than the 2006 cold source intensity, while the winter monsoon index is −0.4545, which is stronger than the 2006 winter monsoon.

Table 1. Composite of different East Asian winter monsoons with strong or weak cold sources over Tibetan Plateau.

Composite Type	Year	The States and Anomaly Value of Q_1	The States and Anomaly of EAWMI
Both strong Q_1 and EAWM	2013	+(1.4892)	+(0.9286)
	2014	+(1.1930)	+(1.5554)
Strong Q_1 and Weak EAWM	2006	+(0.8543)	−(−1.4221)
	2008	+(0.0531)	−(−0.4545)
Both weak Q_1 and EAWM	2015	−(−0.4502)	−(−1.6964)
	2016	−(−0.9035)	−(−1.1955)
Weak Q_1 and Strong EAWM	2010	−(−1.7958)	+(1.2467)
	2017	−(−0.0287)	+(0.6038)

3.3. Atmospheric Circulation and Temperature Analysis

3.3.1. Circulation Features of Different Strong, Weak Winter Monsoon Years and Strong, Weak Cold Source Years

According to the selected four different year types and their corresponding two representative years, a national distribution map of the number of haze days in different years was made using the data of December haze days (Figure 4). It can be seen that under different year types, the distribution of haze days is obviously different. In strong cold source–strong winter monsoon years (2013, 2014, upper left), the haze days in China are the most and widely distributed, and the areas with the most haze days per month are concentrated in the Yangtze River Delta. However, the frequent haze days in the weak cold source–weak winter monsoon years (2015, 2016, right below) are mainly concentrated in the northern part of China, and the haze day phenomenon in Fen-wei Plain is the most obvious under the year type.

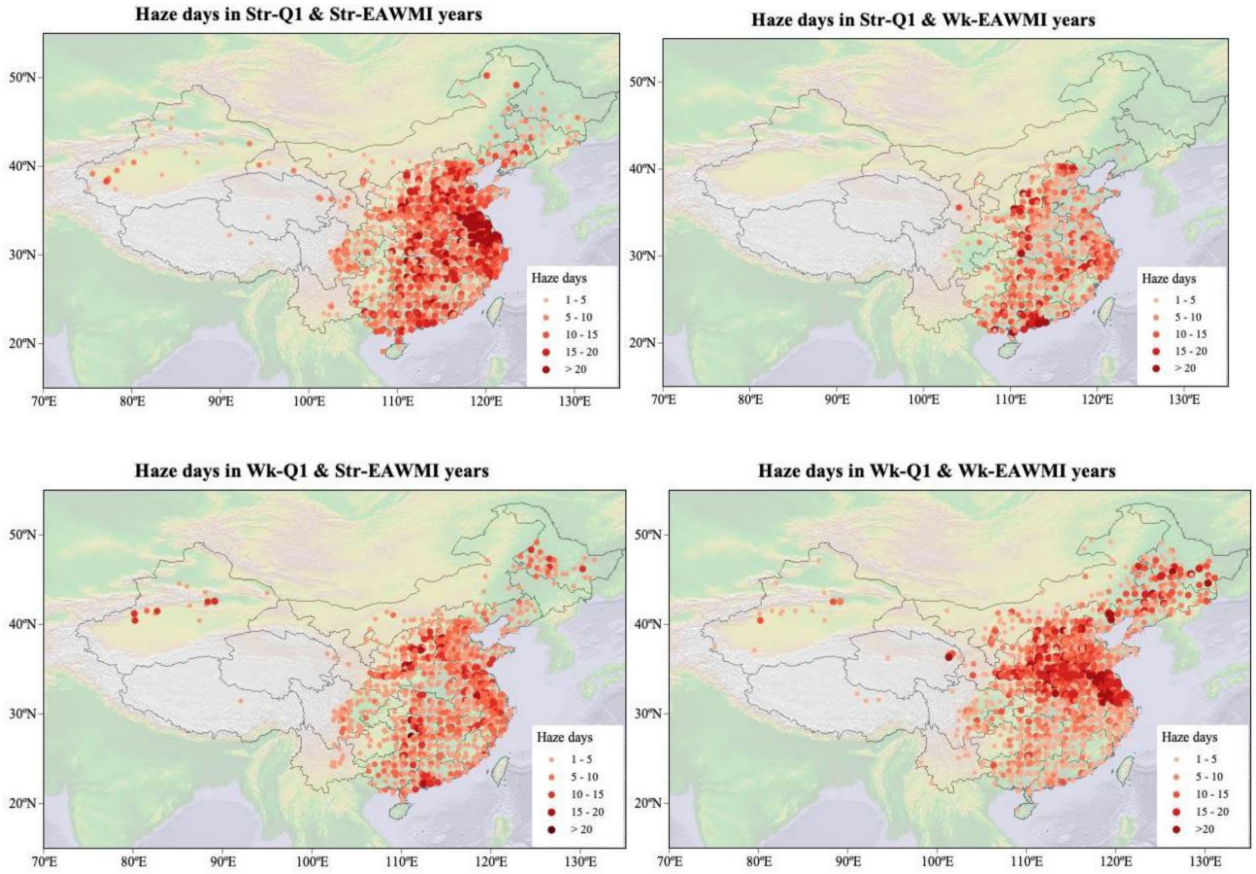

Figure 4. Distribution of haze days under four different combined years with strong, weak cold sources and winter monsoons in China.

For the Pearl River Delta region, the haze phenomenon is more obvious in strong cold source years (upper right) or strong winter monsoon years (lower left), and under the strong cold source superimposed on strong winter monsoon years (upper left), the haze phenomenon in the region is most noticeable, covering the whole Pearl River Delta region. In the Chengdu-Chongqing area, the haze phenomenon is significantly reduced under the strong cold source–weak winter monsoon type (2006, 2008.)

To understand more clearly the difference of circulation background field in the Tibetan Plateau and its surrounding and downstream areas under the above four different year types, cross sections along east–west and south–north directions are drawn, shown in Figure 5. Horizontally, Line1 is drawn along 25° N, Line2 along 30° N and Line3 along 35° N, while, vertically, Line4 is made along 105° E, Line5 along 115° E and Line 6 along 120° E.

(1) Strong Q_1 with strong *EAWMI:* in 2013 and 2014

As shown in Figure 6, in a strong cold source year, there is "temperature inversion cover" in the east of the high terrain, and near the high terrain there is an abnormal uplift airflow. Moreover, the stronger the cold source is, the higher the height of the cooling range in the lower layer. In a strong monsoon year, the cooling range increases from south to north, and the stronger the monsoon, the stronger the cooling degree.

On the north–south section (Figure 7), the temperature over 25–35° N (corresponding to the range of Tibetan Plateau) in the east of the high terrain decreases, and the cold source weakens, causing the reduction in cooling range. In strong winter monsoon years, an abnormally strong northward sinking airflow exists. The stronger the winter monsoon, the stronger the abnormal northerly airflow, accompanied by the northward expansion of the temperature drop range.

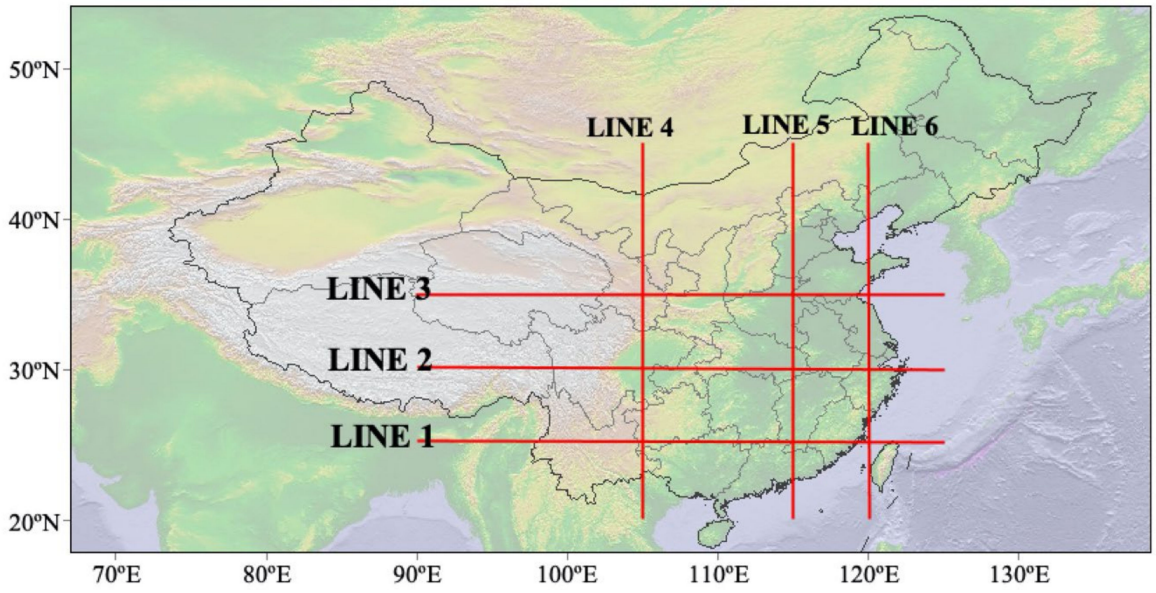

Figure 5. Schematic diagram of cross sections along east–west (LINE1–3) and south–north (LINE4–6) directions.

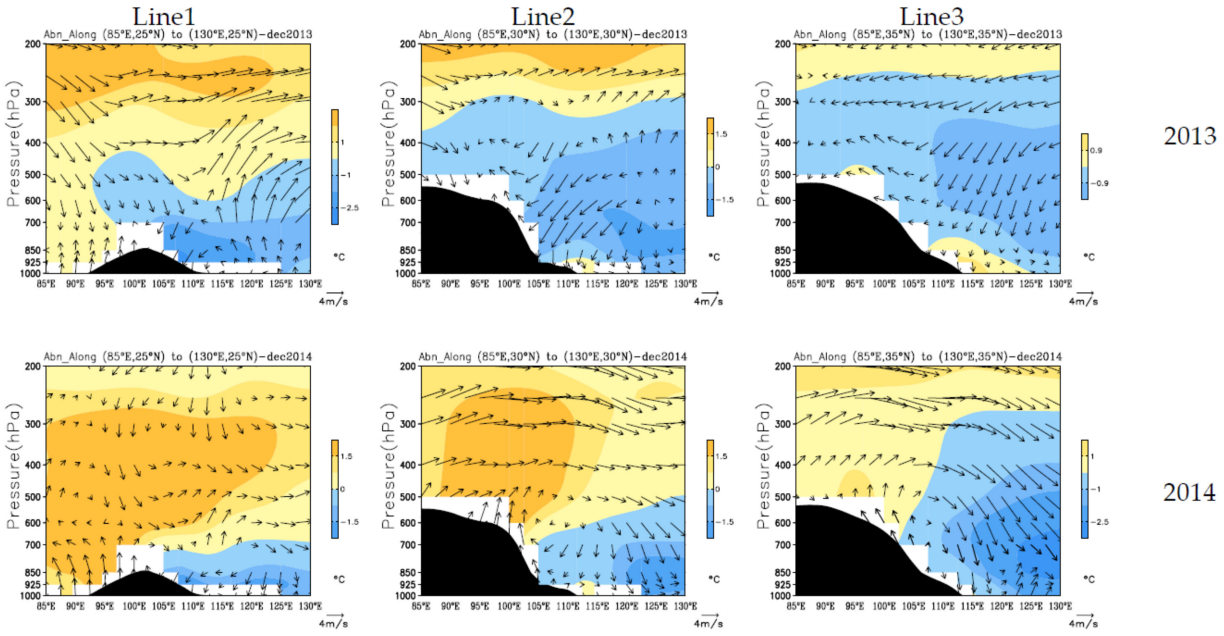

Figure 6. East−west circulation and temperature cross sections of profile 1 (**left**), profile 2 (**middle**) and profile 3 (**right**) in the 2013 (**top**) and 2014 (**bottom**) strong cold source−strong winter monsoon years.

(2) Weak Q_1 with weak *EAWMI*: in 2015 and 2016

It is seen that anomalous easterly downdraft is active near the high terrain. The weaker the cold source becomes, the stronger the temperature rise is in low layers with even larger ranges (Figure 8). And the 25–35° N temperature rises abnormally in the eastern part of the high terrain (except for the area adjacent to the high terrain in 2015). The cooling source is reduced and the temperature rises greatly from 2015 to 2016. As shown in Figure 9, in weak cold source years, the range of abnormal drops in temperature in the eastern part of the high terrain decreases, and even the lower temperature from south to north is unusually high.

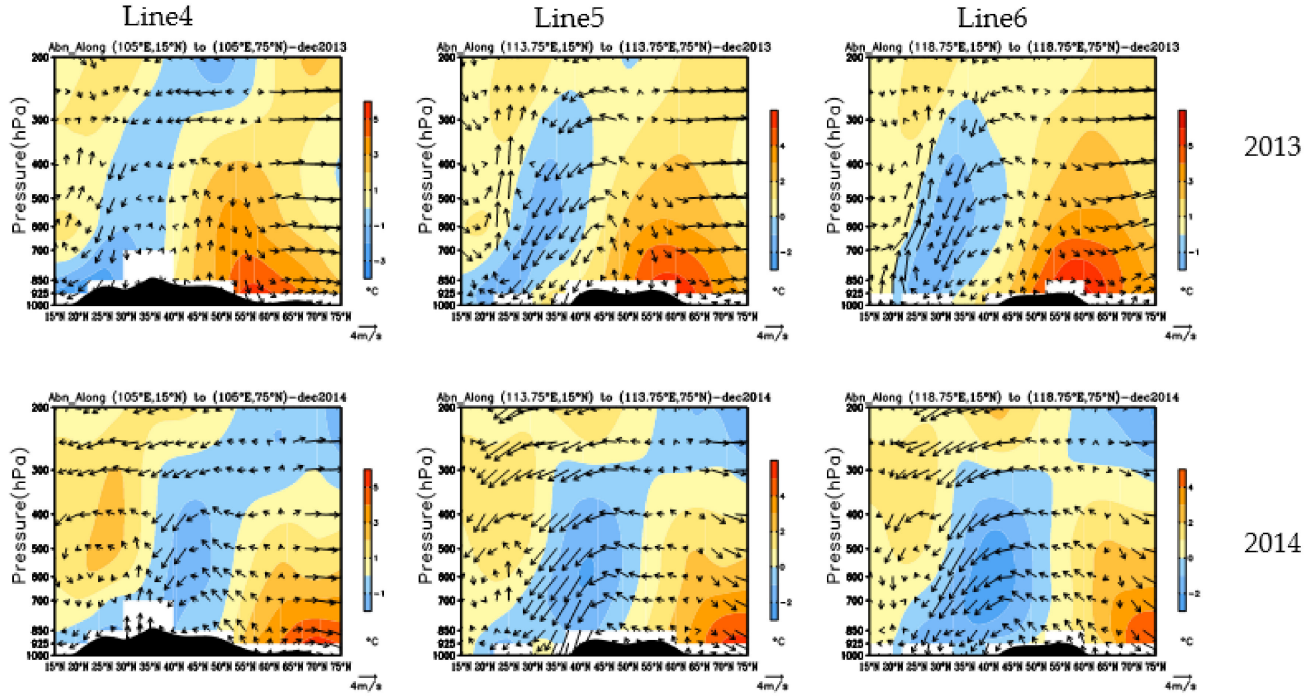

Figure 7. North–south circulation and temperature cross sections of profile 4 (**left**), profile 5 (**middle**) and profile 6 (**right**) in the 2013 (**top**) and 2014 (**bottom**) strong cold source–strong winter monsoon years.

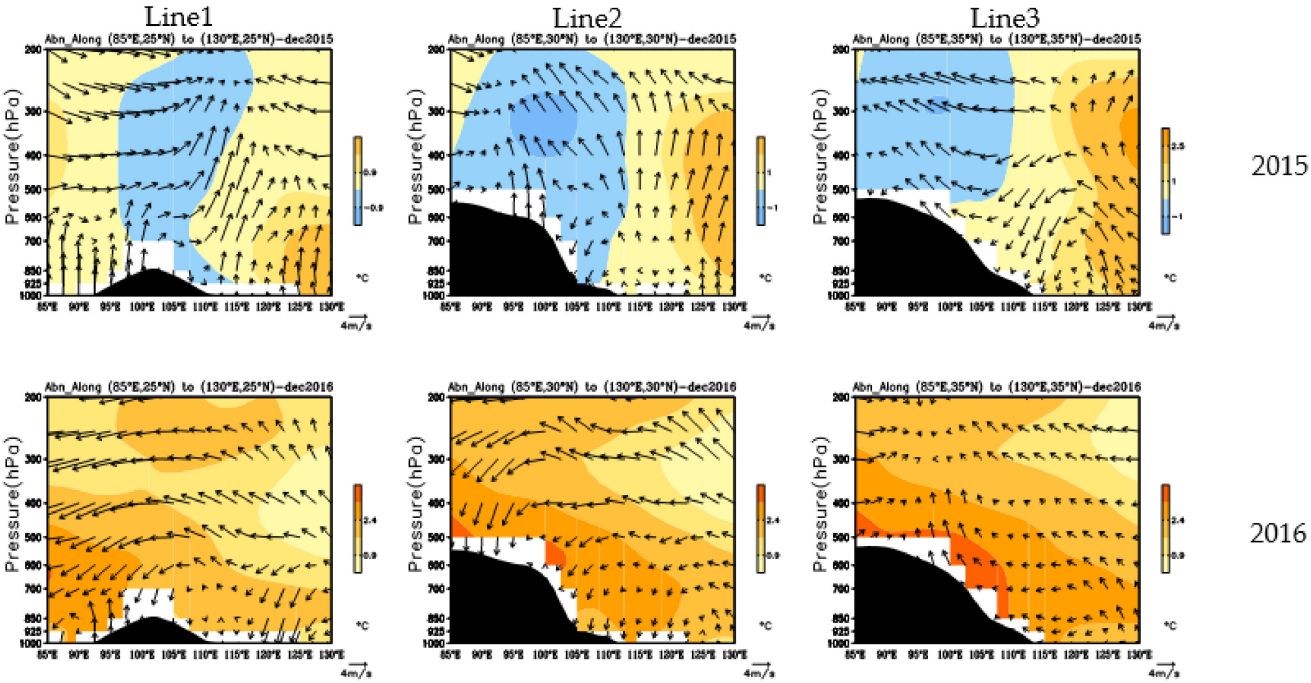

Figure 8. East–west circulation and temperature cross sections of profile 1 (**left**), profile 2 (**middle**) and profile 3 (**right**) in the 2015 (**top**) and 2016 (**bottom**) weak cold source–weak winter monsoon years.

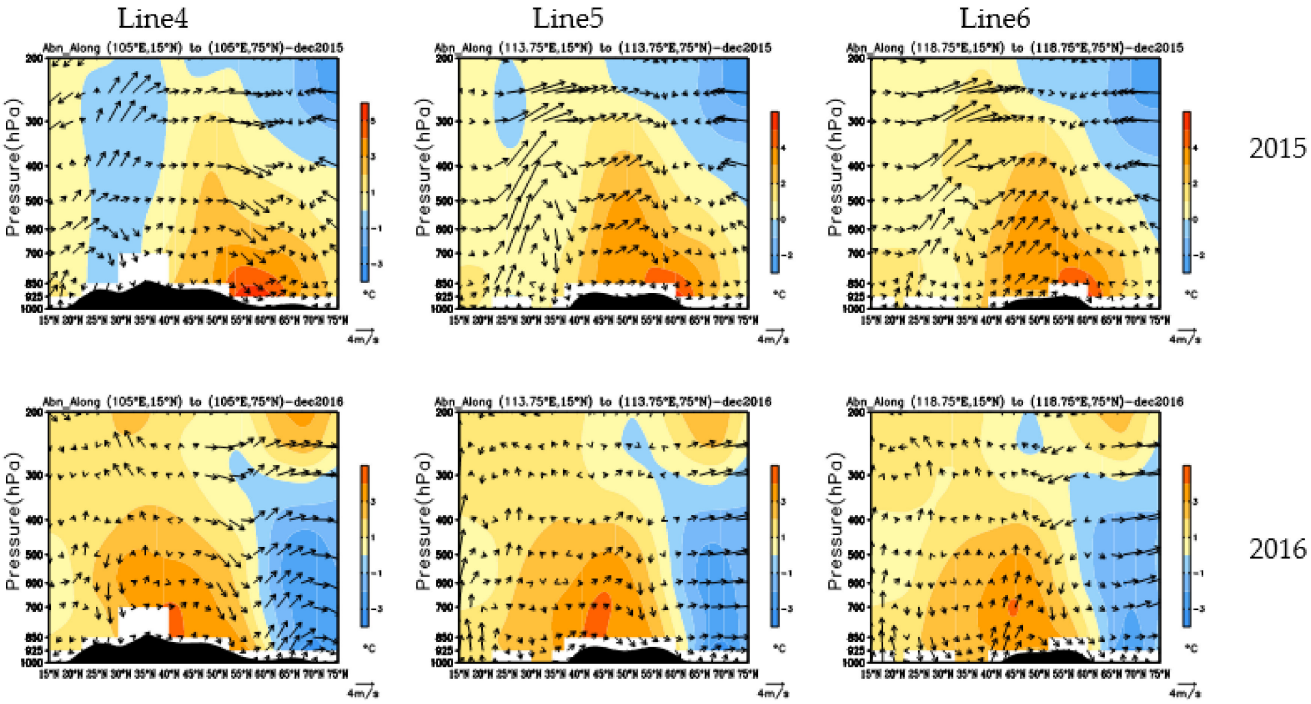

Figure 9. North−south circulation and temperature cross sections of profile 4 (**left**), profile 5 (**middle**) and profile 6 (**right**) in the 2015 (**top**) and 2016 (**bottom**) weak cold source−weak winter monsoon years.

In the years with weak winter monsoon, unusually strong southerly airflows tend to develop. Compared with the 2015 winter monsoon, the monsoon in 2016 was weak. The abnormally southerly wind strengthens and the temperature warming range expands to the north.

(3) Weak Q_1 with Strong *EAWMI*: in 2010 and 2017

In the years of weak cold source (picture omitted), temperature rises in the east of the high terrain, and an abnormal downdraft is apparent in the vicinity of the high terrain. Compared with 2017, the cold source is weakened in 2010, and the westward sinking airflow becomes stronger, which is beneficial for the accumulation of pollutants in the nearby area of the high terrain. As the temperature in the 25–35°N range in the east of high terrain is increased, the temperature rise in the mid-high levels is more obvious when the cold source is enhanced (2017), and, at the same time, the near-surface temperature decreases, resulting in the phenomenon of "temperature inversion cover".

Where temperature decreases there is a clear sinking airflow, which can also be seen from the north–south profile, i.e., within the range of 25–35° N, where cooling and abnormal sinking airflows appear near the ground. The abnormal downdraft is conducive for pollutants to accumulate in the range of 25–35° N far away from the high terrain, leading to increased pollution.

In strong winter monsoon years (picture omitted), the temperature to the east of 35° N decreases significantly, and the westward sinking airflow intensifies. The winter monsoon in 2010 is stronger than in 2017, and the sinking component becomes more remarkable in the middle and high latitudes. On the north–south profile, there is an unusually strong northerly airflow south of 45° N. The stronger the winter monsoon, the stronger the anomalous northerly airflow, accompanied by the expansion of temperature decreasing range in high latitudes, even developing south to the Tibetan Plateau.

(4) Strong Q_1 with weak EAWMI: In 2006 and 2008

We can see that a cooling area hides in the middle and upper atmosphere over the eastern part of high terrain in the strong cold source year (picture omitted). The cold source is stronger in 2006 than in 2008, and there is an abnormally strong updraft near the high

terrain north of 30° N, which helps the vertical diffusion. On the north–south profile, a temperature decreasing area appears above the section of 25–35° N in the east of high terrain. When the cold source is strengthened, the temperature drop range of the upper layer in the area near the high terrain is larger and more obvious, while the temperature drop degree of the area far from the high terrain is weaker.

In the weak monsoon year (picture omitted), there is an abnormal easterly airflow in the lower layers of the middle and low latitudes. In 2006, the winter monsoon is weaker compared to the 2008 winter monsoon. When the monsoon weakens further, the abnormal easterly airflow appears in the middle and high latitudes. On the north–south profile, the abnormal northerly airflow in China's middle and high latitudes weakens, the 2006 winter monsoon is further reduced, and the northerly airflow turns southward. Comparatively, the monsoon in 2008 strengthens and the temperature drops significantly in middle and high latitudes.

For different combinations of strong and weak cold source–winter monsoon years, it can be seen that in strong cold source years, abnormal updrafts appear in areas near high terrain, good for vertical diffusion, while areas far away from high terrain have abnormal downdrafts, which suppress convection. Under the condition that the cold source is strong enough, "temperature inversion cover" will appear in the east of high terrain, which is conducive to further aggravating the pollution with the downdraft away from high terrain areas. However, in weak cold source years, the anomalous updrafts in the near high terrain regions weaken or even change into anomalous downdrafts, which is beneficial to restrain convective diffusion activities in the near high terrain regions.

In strong winter monsoon years (picture omitted), there exists abnormal northerly sinking in mid-high latitudes. The stronger the winter monsoon, the more obvious the temperature drop in mid–high latitudes and the wider the range. By contrast, when the monsoon is weak in winter, the abnormal sinking of northerly wind can turn into a southward flow. The weaker the monsoon, the more obvious the southward flow becomes, accompanied by temperature rises in mid-high latitudes.

3.3.2. Circulation Conditions for Different Regions of China in Different Tibetan Plateau Cold Sources with Strong or Weak Winter Monsoon Years

The Q_1 northeast–southwest boundary determined by the spatial distribution of apparent heat source Q_1 and pollutant correlation coefficients on the Tibetan Plateau (see Figure 6 in Li, Y., et al., 2020.), and the EAWMI north–south boundary (see Figure 6 in Li, Y., et al., 2021.) determined by the spatial distribution of winter monsoon index and pollutant correlation coefficients are respectively marked as Q_1 and EAWMI in Figure 10. For the Q_1 boundary line, the areas to its southeast side tend to experience aggravating pollution when the cold source is stronger, while the pollution increases when the cold source weakens in the areas to its northwest side. For the EAWMI boundary, pollution over the areas to its south side becomes more serious when the East Asian winter monsoon strengthens, but, where it is to the north side of the boundary, weak East Asian winter monsoons can worsen pollution. Therefore, China is divided into four regions, i.e., strong Q_1–strong EAWMI, strong Q_1–weak EAWMI, weak Q_1–strong EAWMI and weak Q_1–weak EAWMI along the two dividing lines, indicating the regional pollution status in the corresponding meteorological characteristic year may be aggravated. Among them, the Beijing–Tianjin–Hebei region is situated in the strong Q_1–weak EAWMI region, the Fen-Wei Plain in the weak Q_1–weak EAWMI region, the Chengdu-Chongqing region in the weak Q_1–strong EAWMI region, and the Pearl River Delta in the strong Q_1–strong EAWMI region. In order to verify the attributes of strong and weak cold sources (winter monsoon), we constructed profile circulation difference maps under different regions and different year types, and analyzed the influence of the atmospheric circulation difference with different year types on the atmospheric pollution in different regions. The representative years selected are: strong Q_1–strong EAWMI year type (2014), weak Q_1–weak EAWMI year

type (2016), strong Q_1–weak EAWMI year type (2006), and weak Q_1–strong EAWMI year type (2010).

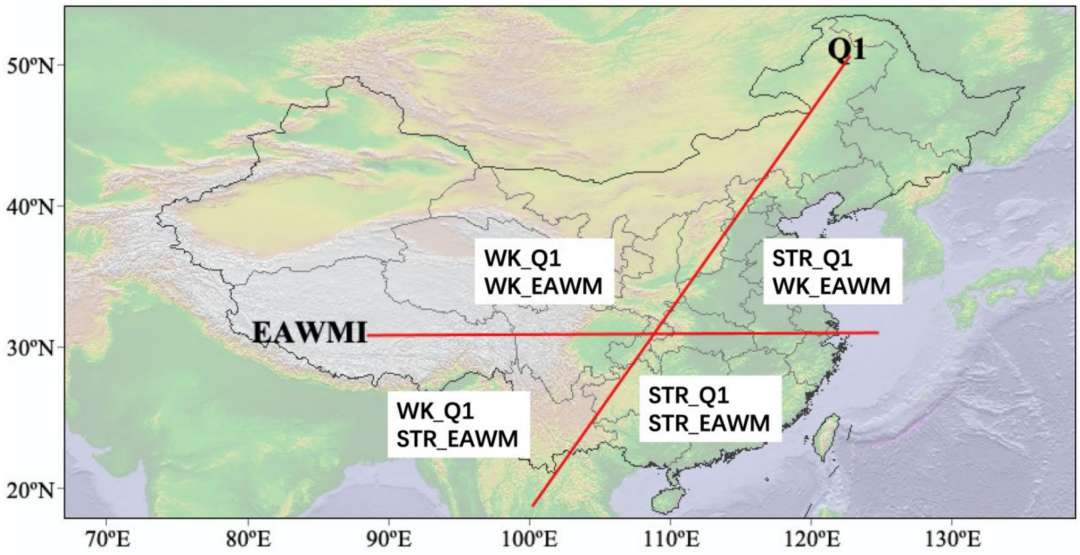

Figure 10. Schematic diagram of different regions in China with the combination of cold sources and strong or weak winter monsoon years.

(1) The Beijing–Tianjin–Hebei region

In weak winter monsoon years (second from left and third from left in Figure 11), there is a southerly updraft in the north–south direction, and an easterly updraft in the east–west direction near the surface in the Beijing–Tianjin–Hebei region (114°–119° E, 36°–41° N). Furthermore, blocked by the topography, the situation is beneficial for the accumulation of pollutants in the Yanshan Mountains. In strong winter monsoon years, the westerly flow in the east–west and the northerly abnormal flow in the north–south are favorable for the outward transportation of pollutants.

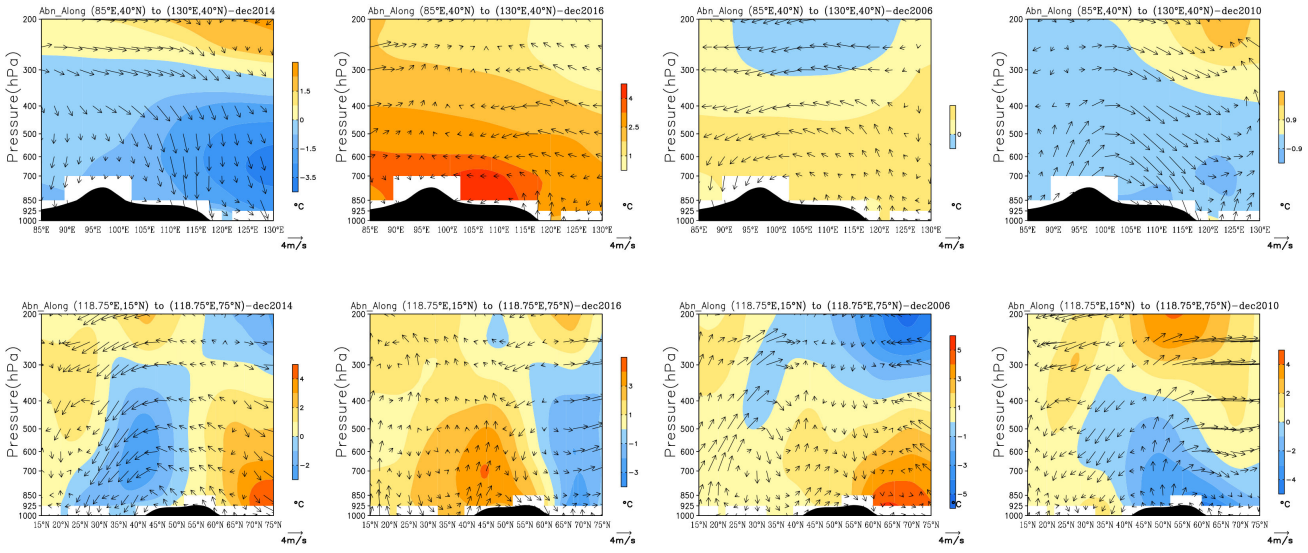

Figure 11. Cross sections of the east−west (**top**) and north−south (**bottom**) circulations and the temperature in strong Q_1−strong EAWMI year (first from left), weak Q_1−weak EAWMI year (second from left), strong Q_1−weak EAWMI year (third from left) and weak Q_1−strong EAWMI year (fourth from left) in Beijing−Tianjin−Hebei region.

However, in years with strong and weak cold sources, the difference in the regional circulation of the Beijing–Tianjin–Hebei region is not as obvious as the difference between strong and weak winter monsoon years. That is, compared with strong and weak cold sources, the difference in winter monsoons has a greater impact on air pollution in the Beijing–Tianjin–Hebei region. When the winter monsoon is weak, the pollution in the Beijing–Tianjin–Hebei region tends to get heaviest.

(2) The Fen-wei Plain region

When the cold source is weak (second from the left: 2016; fourth from the left: 2010; the 2010 cold source is weaker than in 2016 in Figure 12), the ascending component of abnormal airflow in Fenwei Plain (107°–113° E, 34°–39° N) is reduced, even turning into an abnormal downdraft into the plain, conducive to the accumulation of pollutants. When the winter monsoon is weak (second from left: 2016; third from left: 2006; compared to 2016, the 2006 winter monsoon is even weaker), the near-surface airflow is eastward on the east–west profile, which is convenient for the transport of pollutants from Henan Province and other regions into the valley. On the north–south profile, the low-temperature area from the bottom to 400 hPa shrinks northward in 2016, which may be due to the weakening of cold air activity and the weakening of the north wind brought by the cold air going south, so the pollutants in northern China are not prone to spread southward.

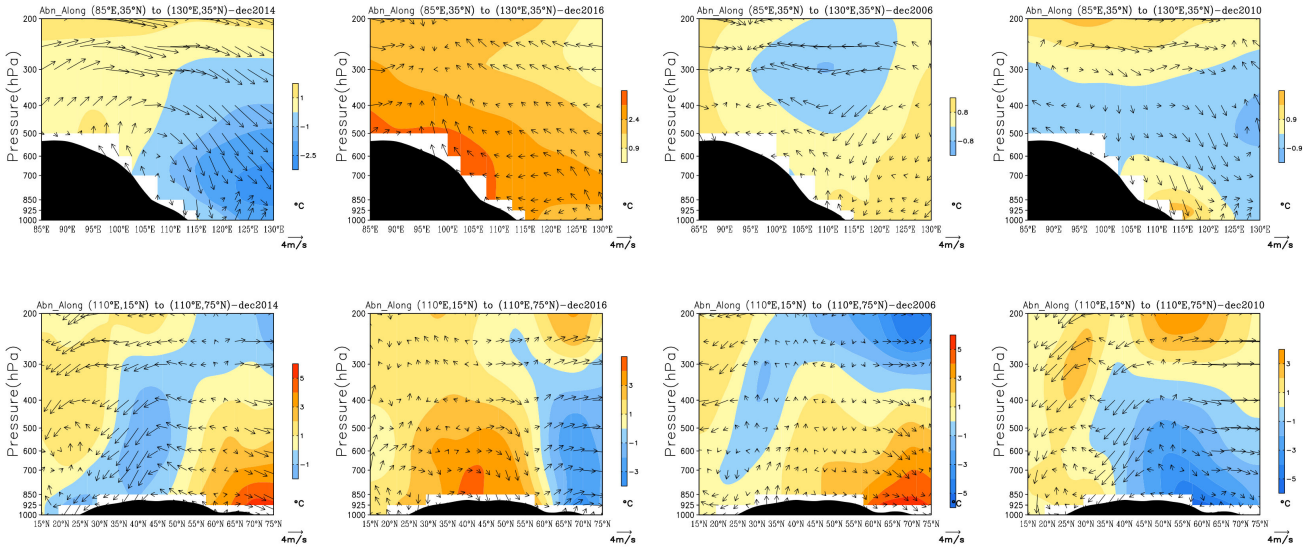

Figure 12. Cross sections of the east−west (**top**) and north−south (**bottom**) circulations and the temperature in strong Q_1−strong EAWMI year (first from left), weak Q_1−weak EAWMI year (second from left), strong Q_1−weak EAWMI year (third from left) and weak Q_1−strong EAWMI year (fourth from left) in the Fen−wei Plain region.

Therefore, the pollution in Fen-wei Plain area is further aggravated by the interaction of weak cold source and weak winter monsoon.

(3) The Chengdu-Chongqing region

In the years with weak cold source, the lower airflows in the east–west direction and the north–south direction over the Chengdu-Chongqing region (around 103–108° E and 28–32° N) show descending airflow. Moreover, the cold source is much weaker in 2010 and the mid-level temperature warming in the east side of the high terrain is weaker than that in 2016. As a result, more consistent downdrafts appear, helping restrain convection and diffusion and resulting in more serious pollution. In the years with strong monsoon (picture omitted), the near-surface has northerly sinking flow in the north–south direction, and if the monsoon is strong enough, abnormal easterly airflow occurs in the east–west direction, able to transport the pollutants from the east into the basin. Furthermore, combined with the blocking effect of topography, the basin pollution is intensified.

Therefore, the combination of weak cold source and strong monsoon is more conducive to the accumulation of pollution in the basin.

(4) The Pearl River Delta region

During strong winter monsoon years, the near-surface layer of the Pearl River Delta (near 112–116° E, 22–25° N) flows a northerly downdraft in the north–south direction, and there is a westward flow east–west, which is propitious to transporting and accumulating pollutants to the Pearl River Delta region from the north and west. In 2014, when the cold source is strong enough, a "temperature inversion cover" is formed at high altitudes on the east–west profile, which is beneficial to inhibit the local convection and diffusion (picture omitted).

Therefore, in the strong monsoon years, the pollution in the Pearl River Delta region tends to be aggravated, and then with the strong cold source conditions, pollution can become worse.

(5) The Yangtze River Delta region

In years with cold sources strong enough (picture omitted), a westerly downdraft exists in the near-surface of the Yangtze River Delta region, causing the pollutants to be transported to the delta from the western region and accumulated. Moreover, when the cold source is strong enough, "temperature inversion cover" can be formed in the upper air in the east–west profile, conducive to the suppression of local convective diffusion.

In strong winter monsoon years, the near-surface layer of the Yangtze River Delta has northerly descending flow in the north–south direction, and westerly flow in the east–west direction. Such conditions are favorable for transporting and accumulating pollutants from the north and west areas to the Yangtze River Delta.

Therefore, affected by the combination of strong cold source and strong winter monsoon, atmospheric pollution in the Yangtze River Delta is the most serious.

3.3.3. $PM_{2.5}$ Mass Concentration in December 2013–2017 in Typical Regional Years in China

From 2013 to 2017, presenting different Q_1 and EAWMI characteristics, both 2013 and 2014 were strong Q_1 and strong EAWM years. Between the two years, the cold source in 2013 was stronger than that in 2014, while the EAWM was slightly weaker than that in 2014. Both 2015 and 2016 were weak Q_1 and weak EAWM years. Between the two, the cold source in 2016 was weaker than that in 2015, and the EAWM in 2015 was slightly stronger than that in 2016. Then, 2017 was a weak Q_1 and strong EAWM year, and its Q_1 anomaly value was -0.0287, slightly lower than the annual average.

Based on the observation data of $PM_{2.5}$ mass concentration from December 2013 to December 2017, an annual $PM_{2.5}$ time series diagram for each region was made, as shown in Figure 13. As can be seen from the figure, the 2013–2017 PM2.5 mass concentration in the Beijing–Tianjin–Hebei region is generally higher than in other regions. During 2015–2016, the weak winter monsoon years, air pollution is the most severe, and moreover with weaker winter monsoon in 2015 than in 2016, the $PM_{2.5}$ value in 2015 is much higher.

For the Fen-wei Plain, pollution is usually serious in the weak cold source and weak winter monsoon years, corresponding to 2015–2016, but the pollution in 2014 is the lightest, for it is a strong cold source and strong winter monsoon year.

The $PM_{2.5}$ mass concentration in the Pearl River Delta region from 2013 to 2017 is the lowest among the five regions. Pollution is the heaviest when the winter monsoon is strong, as seen in 2013, 2014, and 2017. On the contrary, in the years with the weakest winter monsoon (2015), pollution is the lightest.

In the above discussion, heavy pollution occurs in the Chengdu-Chongqing area in the years when cold source is weak and winter monsoon is strong. However, from 2013 to 2017, such a condition did not form in any years. In 2015 and 2016, the cold sources and winter monsoon were both weak, but the 2016 monsoon increased its strength, causing the pollution in this region to worsen.

The Yangtze River Delta region suffers from the heaviest pollution in years with strong cold sources and strong winter monsoons, corresponding to 2013–2014. This region

happens to be located in the EAWMI boundary area. In the years when the winter monsoon is particularly strong, the northerly wind is abnormally strong, which may push the boundary line to move southward. At this time, the Yangtze River Delta is situated to the north side of the boundary, showing the characteristics of the stronger (weak) winter monsoon and the weaker (stronger) pollution. If the strong winter monsoon is relatively weak, the Yangtze River Delta will experience increased pollution and vice versa.

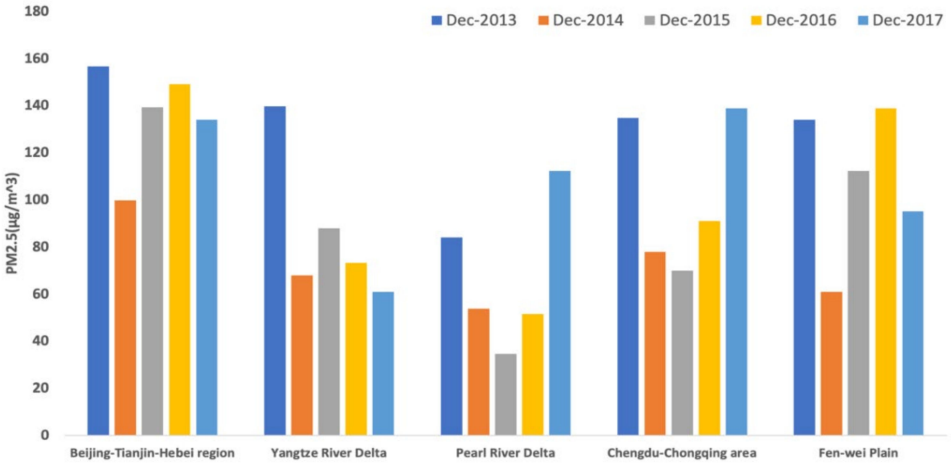

Figure 13. Comparison of $PM_{2.5}$ observations in China's five typical regions in December of 2013–2017.

4. Summary and Discussion

Comparing different combinations of strong/weak cold sources and winter monsoon years, we found that when the cold source is strong, abnormal ascending airflows appear in the areas near high terrain, conducive to vertical diffusion, while in the areas far away from high terrain there are abnormal downdrafts, inhibiting convective activities. In the case with strong enough cold sources, "temperature inversion cover" will build in the east of high terrain, cooperating with the descending airflow away from the high terrain and further aggravating the pollution. However, in weak cold source years, the abnormal updrafts in the near high terrain areas are weakened or even transformed into abnormal sinking airflow, which is beneficial to suppress the convection and diffusion activities in the near high terrain area. Furthermore, under the influence of southerly winds, pollutants from India and surrounding areas will be transported to the Qinghai-Tibet Plateau [32–35]. These pollutants will probably be transported to eastern China in strong cold source years, which may further affect the pollution of different typical pollutant areas in China, which requires more follow-up research and analysis to discuss.

In strong winter monsoon years, the lower layers of mid-high latitudes have abnormal descending northerly airflow, and the stronger the winter monsoon, the more obvious the temperature drop in mid-high latitudes and the wider the range. In contrast, when the winter monsoon is weak, the abnormal northerly flow can turn into a southerly airflow. The weaker the monsoon, the stronger the southerly airflow, accompanied by the temperature rise in mid-high latitudes.

The aggravation of pollution in the Beijing–Tianjin–Hebei region is primarily affected by the southerly and easterly updrafts. In addition, the blocking effect of the topography makes pollutants accumulate in the Yanshan Mountains. Compared with the impact of cold sources, variations of winter monsoon have more significant influence on the atmospheric pollution in the Beijing–Tianjin–Hebei region. In the weak winter monsoon years, the pollution in the region is most serious.

In the Fen-wei Plain, when the cold source is weak and the winter monsoon is weak, there are abnormal sinking airflows into the plain. There are easterly airflows in the east–

west near-surface, which is conducive to transporting pollutants from Henan and other places to the valley, and to further aggravate the pollution in Fen-wei Plain.

Over the Chengdu-Chongqing area, when the weak cold source is combined with a strong winter monsoon, the circulation situation is conducive to aggravation of pollution, because consistent sinking airflows occur in the east side of the high terrain at that time, and the low-level abnormal easterly flows, along with strong winter monsoon, bring pollutants from the east into the basin. Furthermore, the obstruction by the high terrain further aggravates the pollution situation.

The pollution condition in the Pearl River Delta region is the same as that in the Yangtze River Delta region. In the strong cold source with strong winter monsoon year, pollution tends to get worse, because it blows a northerly descending flow north–south and westerly flow east–west, which is favorable for the pollutants from northern and western regions to be transported into the region and accumulated. Furthermore, when the cold source is strong enough, "temperature inversion cover" exists high in the sky, which is beneficial to inhibit local convection diffusion, further increasing pollution.

Author Contributions: Conceptualization, X.A. and B.W.; methodology, C.W. and Y.L.; validation, Y.L.; formal analysis, Y.L.; investigation, X.A.; resources, X.A.; data curation, C.W. and Y.L.; writing—original draft preparation, Y.L.; writing—review and editing, X.A.; visualization, X.A.; supervision, B.W. and J.L.; project administration, X.A.; funding acquisition, X.A. All authors have read and agreed to the published version of the manuscript.

Funding: This research was supported by the Key project of Scientific and Technological Research Program of Chongqing Municipal Education Commission (KJZD-K201901403), the National Natural Science Foundation of China (41975173), China, and the General project of Natural Science Foundation of Chongqing Bureau of Science and Technology (cstc2019jcyj-msxmX0879).

Data Availability Statement: Not applicable.

Acknowledgments: The authors would like to thank the editors for assistance in enhancing the quality of the present paper, as well as the reviewers for their kind and precious work. Special thanks to An for her support, feasibility analysis and knowledge sharing in recent years.

Conflicts of Interest: The authors declare no conflict of interest.

References

1. Ding, Y.; Liu, Y.; Liang, S.; Ma, X.; Zhang, Y.; Si, D.; Liang, P.; Song, Y.; Zhang, J. Interdecadal Variability of the East Asian Winter Monsoon and Its Possible Links to Global Climate Change. *J. Meteor. Res.* **2014**, *28*, 693–713. [CrossRef]
2. Pei, L.; Yan, Z.; Chen, D.; Miao, S. Climate variability or anthropogenic emissions: Which caused Beijing Haze? *Environ. Res. Lett.* **2020**, *15*, 034004. [CrossRef]
3. Tagaris, E.; Liao, K.J.; DeLucia, A.J.; Deck, L.; Amar, P.; Russell, A.G. Potential impact of climate change on air pollution related human health effects. *Environ. Sci. Technol.* **2009**, *43*, 4979–4988. [CrossRef] [PubMed]
4. Qin, Z.; Sun, Z. Influence of Abnormal East Asian Winter Monsoon on the Northwestern Pacific Sea Temperature. *Chin. J. Atmos. Sci.* **2006**, *30*, 257–267. [CrossRef]
5. Pu, Y.; Pei, S.Q.; Li, C.Y.; Chen, Y. Influence of Anomalous East Asian Winter Monsoon on Zonal Wind Anomalies over the Equatorial Western Pacific. Chin. *J. Atmos. Sci.* **2006**, *30*, 69–79. [CrossRef]
6. Liu, S.; Sui, B.; Li, J.; Tu, G. Influence of East Asian Winter Monsoon on Winter Air Temperature in Northeast China. *Sci. Geogr. Sin.* **2015**, *35*, 507–514.
7. Chen, Y.; Jiang, W.M.; Guo, W.L.; Miao, S.G.; Chen, X.Y.; Ji, C.P.; Wang, X.Y. Study on the effect of the city group development in Pearl River Delta on local air pollutant dispersion by numerical modeling. *Acta Sci. Circumstantiae* **2005**, *25*, 700–710. (In Chinese)
8. Ye, D.; Gao, Y. *Qinghai-Tibet Plateau Meteorology*; Science Press: Beijing, China, 1979. (In Chinese)
9. Flohn, H. Large-scale aspects of the "summer monsoon" in South and East Asia. *J. Meteor. Soc. Jpn.* **1957**, *75*, 180–186. [CrossRef]
10. Wang, T.; Wu, G.; Wan, R. The influence of the thermal and dynamic effects of the Qinghai-Tibet Plateau on the circulation of the Asian monsoon region. *J. Plateau Meteor.* **2008**, *1*, 1–9. (In Chinese)
11. Li, G. *Dynamic Meteorology of the Qinghai-Tibet Plateau*; Meteor Press: Beijing, China, 2002. (In Chinese)
12. Wu, G.; Zhang, Y. Thermal and mechanical forcing of the Qinghai-Tibet Plateau and the onset of the Asian monsoon*I. Location of the outbreak. *J. Chin. J. Atmos. Sci.* **1998**, *6*, 22–35. (In Chinese)
13. Wu, G.; Liu, Y.; Liu, X.; Duan, A.; Liang, X. How does the heating of the Qinghai-Tibet Plateau affect the Asian summer climate pattern. *Chin. J. Atmos. Sci.* **2005**, *1*, 47–56, 167–168. (In Chinese)

14. Wang, Q. *The Relationship between the Climatic Characteristics and Anomalies of the Qinghai-Tibet Plateau Heat Source in Spring and the Atmospheric Circulation and My Country's Climate*; Nanjing University of Information Science and Technology: Nanjing, China, 2006. (In Chinese)
15. Charney, J.; Eliassen, A. A Numerical Method for Predicting the Perturbations of the Middle Latitude Westerlies. *Tellus* **1949**, *1*, 38–54. [CrossRef]
16. Pan, B.; Li, J. The Qinghai-Tibet Plateau: The Driver and Amplifier of Global Climate Change—III. The impact of the uplift of the Qinghai-Tibet Plateau on climate change. *J. Lanzhou Univ.* **1996**, *1*, 108–115. (In Chinese)
17. Hahn, D.; Manabe, S. The role of mountains in the south Asian monsoon circulation. *J. Atmos. Sci.* **1975**, *32*, 1515–1541. [CrossRef]
18. Li, G.; Gu, W. The influence of the Tibetan Plateau heat source anomalies on the circulation and precipitation in North China. *Shandong Meteor.* **2013**, *2*, 1–4. (In Chinese)
19. Gao, H. The East Asian Winter Monsoon Index and Its Characterization of East Asian Atmospheric Circulation Anomalies. *Acta Meteor. Sin.* **2007**, *2*, 272–279. (In Chinese)
20. Ma, F.; Guan, Z. The distribution characteristics of winter AOD in eastern China and its possible connection with winter monsoon circulation. *Acta Atmos. Sci.* **2019**, *42*, 255–266. (In Chinese)
21. Xu, J.; Zhu, Q.; Shi, N. The relationship between the East Asian winter monsoon and the ENSO cycle and its decadal anomalies in the past 100 years. *Chin. J. Atmos. Sci.* **1997**, *6*, 2–9. (In Chinese)
22. Li, Y.; An, X.; Fan, G.; Wang, C.; Zhao, Y.; Li, J. Influence of Thermal Effects on Qinghai-Tibet Plateau on Air Quality in Typical Regions of China in Winter. *Atmosphere* **2020**, *11*, 50. [CrossRef]
23. Li, Y.; An, X.; Zhang, P.; Yang, J.; Wang, C.; Li, J. Influence of East Asian winter monsoon on particulate matter pollution in typical regions of China. *Atmos. Environ.* **2021**, *260*, 118213. [CrossRef]
24. Yu, Y.; Zhang, Z.; Feng, M. *National Meteorological Information Center Haze Data Collection (V1.0), Internal Data of National Meteorological Information Center*; National Meteorological Information Center: Beijing, China, 2013.
25. Zhong, S.; He, J.; Guan, Z.; Wen, M. Climatic characteristics of atmospheric heat sources on the Qinghai-Tibet Plateau from 1961 to 2001. *Acta Meteor. Sin.* **2009**, *67*, 407–416. (In Chinese)
26. Huang, X.; Xiao, D.; Jiao, M.; Li, Y. Climate characteristics of atmospheric heat sources on the Qinghai-Tibet Plateau in the past 30 years. *Plateau Mt. Meteor. Res.* **2014**, *34*, 38–43. (In Chinese)
27. Luo, X.; Xu, J. Atmospheric heat sources on the Qinghai-Tibet Plateau and uncertainty factors in their estimation. *Adv. Clim. Chang. Res.* **2019**, *15*, 33–40. (In Chinese)
28. Yanai, M.; Li, C.; Song, Z. Seasonal heating of the Tibetan plateau and its effects on the evolution of the Asian summer monsoon. *J. Meteor. Soc. Jpn.* **1992**, *70*, 319–351. [CrossRef]
29. Sun, B.; Li, C. Relationship between the disturbances of East Asian trough and tropical convective activities in boreal winter. *Chin. Sci. Bull.* **1997**, *42*, 500–504. (In Chinese)
30. Xu, X.; Chen, L. Research progress on the Qinghai-Tibet Plateau atmospheric science experiment. *J. Appl. Meteor. Sci.* **2006**, *6*, 756–772.
31. Zhang, R.; Wang, Y.; He, Q.; Chen, L.; Zhang, Y.; Qu, H.; Smeltzer, C.; Li, J.; Alvarado, M.A.L.; Vrekoussis, M.; et al. Enhanced trans-Himalaya pollution transport to the Tibetan Plateau by cut-off low systems. *Atmos. Chem. Phys.* **2017**, *17*, 3083–3095. [CrossRef]
32. Lawrence, M.G.; Lelieveld, J. Atmospheric pollutant outflow from southern Asia: A review. *Atmos. Chem. Phys.* **2010**, *10*, 11017–11096. [CrossRef]
33. Kopacz, M.; Mauzerall, D.L.; Wang, J.; Leibensperger, E.M.; Henze, D.K.; Singh, K. Origin and radiative forcing of black carbon transported to the Himalayas and Tibetan Plateau. *Atmos. Chem. Phys.* **2011**, *11*, 2837–2852. [CrossRef]
34. Lu, Z.; Streets, D.G.; Zhang, Q.; Wang, S. A novel back trajectory analysis of the origin of black carbon transported to the Himalayas and Tibetan Plateau during 1996–2010. *Geophys. Res. Lett.* **2012**, *39*, L01809. [CrossRef]
35. Zhao, Z.; Cao, J.; Shen, Z.; Xu, B.; Zhu, C.; Chen, L.W.A.; Su, X.; Liu, S.; Han, Y.; Wang, G.; et al. Aerosol particles at a high-altitude site on the Southeast Tibetan Plateau, China: Implications for pollution transport from South Asia. *J. Geophys. Res. Atmos.* **2013**, *118*, 11360–11375. [CrossRef]